

Plagioclase-melt equilibria in hydrous systems

TODD B. HOUSH,* JAMES F. LUHR

Department of Earth and Planetary Sciences, Washington University, St. Louis, Missouri 63130, U.S.A.

ABSTRACT

Although plagioclase is the most common mineral in crustal rocks, plagioclase-melt equilibrium relationships in hydrous silicate systems are poorly understood. This study is based on analyses of 54 new plagioclase-melt pairs produced in H₂O-saturated experiments on natural andesite and basalt in the pressure range of 1–4 kbar. We combined these data with H₂O-saturated data from the literature, and we evaluated the quality of available activity-composition models for silicate melts by calculating equilibrium constants for the exchange of albite and anorthite components between plagioclase and melt as functions of reciprocal temperature. Plagioclase-melt equilibrium relationships are shown to be strongly dependent on both the temperature and the H₂O content of the melt. Because the H₂O content of natural melts is generally not known, we present two expressions that relate the temperature of the system to the H₂O content of the melt, one for albite exchange and the other for anorthite exchange. Successful application of these relationships to natural rocks requires both a good estimate of preeruptive temperature and knowledge of the equilibrium plagioclase and melt compositions. Under optimal conditions, the uncertainties in estimated H₂O contents are 0.54 and 0.33 wt% for the albite and anorthite exchange equations, respectively.

INTRODUCTION

Plagioclase is the most common mineral found in igneous rocks and crystallizes from silicate melts over a wide range of temperatures, pressures, and H₂O contents. Bowen (1913) demonstrated the form of the liquidus-solidus loop in the system albite-anorthite at 1 bar, and Yoder et al. (1957) showed the strong thermal depression of the loop, with little change in shape, at 5-kbar H₂O pressure. These relationships pointed toward the possibility of using the compositions of coexisting plagioclase and glass in volcanic rocks to deduce the temperature of equilibration and the H₂O content of the melt. This important goal has remained elusive largely because of a paucity of experimental plagioclase-glass pairs for H₂O-bearing natural compositions and because of limitations in available activity-composition models for silicate melts. Recent years have seen the publication of coexisting phase compositions for a significant number of hydrous experimental charges (Helz, 1976; Baker and Eggler, 1987; Rutherford et al., 1985; Conrad et al., 1988), along with a variety of models for silicate melts (Ghiorso et al., 1983; Nielsen and Dungan, 1983; Burnham and Nekvasil, 1986). This study is based on a set of 54 plagioclase-melt pairs produced in H₂O-saturated experiments using natural andesites and basalts in the pressure range of 1–4 kbar. We combined these data with H₂O-saturated pairs from

Rutherford et al. (1985) in order to evaluate the available activity-composition models for silicate melts by calculating equilibrium constants for exchange of albite and anorthite components between melt and plagioclase as functions of reciprocal temperature. We present expressions that can be used to calculate the H₂O contents of melts from natural plagioclase-glass pairs if the temperature can be independently estimated.

PREVIOUS WORK

A variety of plagioclase-melt geothermometers have been proposed that are applicable to low-pressure, anhydrous conditions. These geothermometers are based upon the rather extensive set of coexisting plagioclase-melt pairs from experimental studies at 1-bar pressure. These geothermometers primarily differ in the nature of the activity-composition model adopted for the silicate melt and include purely empirical formulations (Smith, 1983; Glazner, 1984), two-site quasi-lattice models (Drake, 1976; Nielsen and Dungan, 1983), and the regular-solution model of Ghiorso et al. (1983). These geothermometers calibrated at 1 bar are generally able to predict temperatures of plagioclase-melt equilibration to within 10–30 °C.

Relatively few models have been proposed for equilibria between plagioclase and hydrous silicate melts. Best known are the model of Kudo and Weill (1970) and its subsequent modification by Mathez (1973, 1974). The Kudo-Weill formulation assumed a regular-solution model for the silicate melt and was calibrated using phase

* Present address: Department of Earth, Atmospheric, and Planetary Sciences, Massachusetts Institute of Technology, Cambridge, Massachusetts 02139, U.S.A.

TABLE 1. Major element analyses of starting materials

St. comp. Technique:	A1 XRF	G XRF	B XRF	A2 WC
	(wt%)			
SiO ₂	57.53	58.60	52.33	60.07
TiO ₂	0.71	0.00	0.84	0.64
Al ₂ O ₃	18.95	18.18	16.13	17.91
Fe ₂ O ₃ *	6.60	6.15	8.30	5.81
MnO	0.19	0.00	0.14	0.11
MgO	2.27	2.15	9.37	3.04
CaO	7.14	6.64	8.39	5.94
Na ₂ O	4.12	4.77	3.31	4.64
K ₂ O	2.82	2.85	0.72	1.34
P ₂ O ₅	0.38	0.00	0.13	0.20
Total	100.71	99.34	99.66	99.70
	CIPW norm (wt%)			
q	3.80	2.11	0.00	9.46
or	16.67	16.84	4.26	7.92
ab	34.86	40.36	28.01	39.26
an	24.89	19.78	27.03	24.09
di	6.71	11.00	11.04	3.34
hy	9.12	6.97	18.85	11.79
ol	0.00	0.00	5.51	0.00
mt	1.91	1.78	2.41	1.68
il	1.35	0.00	1.60	1.22
ap	0.88	0.00	0.30	0.46

Note: St. comp. = starting compositions A1, G, B, and A2 as described in the text. A2 was not converted to glass; it was loaded into capsules as fine rock powder. Technique: XRF = X-ray fluorescence analysis of glass disk prepared from fusion using a ratio of nine parts lithium tetraborate to one part glass or gel mix; WC = wet chemistry (analyst, I.S.E. Carmichael). CIPW norms calculated assuming $Fe^{3+}/(Fe^{3+} + Fe^{2+}) = 0.2$

* Total Fe as Fe₂O₃.

relations in synthetic systems at 1-bar pressure (Bowen, 1913, 1915; Prince, 1943), unpublished data for H₂O-saturated granitic compositions at 500 and 1000 bars pressure, and 5-kbar data for the H₂O-saturated albite-anorthite binary (Yoder et al., 1957). As discussed below, the Kudo-Weill model performs poorly in predicting the known H₂O pressures for the experimental data used in this study, pointing to the need for reformulation of a plagioclase-melt geothermometer.

EXPERIMENTAL DESIGN

The materials studied and experimental techniques are described in detail by Luhr (1990) and will be discussed only briefly here. The experiments were performed at the U.S. Geological Survey in Reston, Virginia, using an internally heated pressure vessel with Ar gas as the pressure medium. Most experiments were conducted using a grid-like array of temperature (800, 850, 900, 950, and 1000 °C) and pressure (2 and 4 kbar) conditions. Fewer experiments were conducted at pressures of 1 and 2.5 kbar. Temperatures reported in this study are believed to be accurate to ±3 °C, and pressures are probably accurate to ±50 bars. Oxygen fugacity was buffered using one of three different H₂O-saturated solid O buffers in a double Au capsule arrangement: FMQ, fayalite-magnetite-quartz; MNH, manganosite-hausmanite; and MTH, magnetite-hematite.

Four different starting compositions from the subduction-related Mexican Volcanic Belt were studied: A1, El

Chichón trachyandesite erupted in 1982 (Luhr et al., 1984); G, a synthetic gel corresponding to a Ti-Mn-P-free equivalent of the 1982 trachyandesite; B, Jorullo basalt JOR-44 erupted in 1759 (Luhr and Carmichael, 1985); and A2, andesite COL-40 erupted from Volcán Colima in 1975 (Luhr and Carmichael, 1990). As described in Luhr (1990), compositions A1 and B were converted to glasses at 1 bar, and these glasses were used in the experiments. Major element compositions and CIPW norms for the A1 and B glasses, the gel G, and the rock powder of A2 are given in Table 1. For compositions A1, G, and B, S was added to the ground glass or gel (3 wt% SO₃) in the form of the stable S-bearing mineral: pyrrhotite for the FMQ buffer and anhydrite for the MNH and MTH buffers. S was not added to composition A2, which contains only the natural sulfur content of approximately 0.1 wt% equivalent SO₃. Prior to crimping and welding of loaded sample capsules, distilled H₂O was added in quantities sufficient to assure vapor saturation at the experimental pressure: 5 wt% H₂O at 1 kbar, 10 wt% at 2 kbar and 2.5 kbar, and 15 wt% at 4 kbar. Fugacities of all important gas species at experimental conditions for samples of compositions A1, G, and B are given in Luhr (1990). Although these samples are S bearing, fugacities of all S gas species were less than 15 bars in all sample assemblies, and the samples were close to the condition $P_{H_2O} = P_{total}$. The vapor phase for the nearly S-free composition A2 was essentially pure H₂O. The duration of each experiment in hours, and the temperature, pressure, and O buffer are listed in Table 2. All experiments were conducted as crystallization experiments, with temperature first taken to 1000 °C for 30 min, followed by manual cooling to the temperature of the experiment at an approximate rate of 200 °C/h. This technique generally produced relatively coarse-grained (10 to >100 μm) textures of homogeneous phases that were ideal for analysis of both glass and crystals. Phase assemblages for all charges of compositions A1, G, and B are given in Luhr (1990). Backscattered electron images of representative plagioclase and glass textural relationships for each of the four starting compositions are shown in Figure 1.

MICROPROBE TECHNIQUES

The experimental glasses were analyzed using the ARL-SEMQ electron microprobe at the U.S. Geological Survey, Reston, Virginia. Analytical techniques and corrections for alkali loss are discussed in Luhr (1990). Ten to 12 individual spot analyses were typically collected for glass in each experimental sample. Spatially related compositional variations were not detected in any sample. The number of spots analyzed and mean and one standard deviation values are listed in Luhr (1990).

Plagioclase was analyzed on two different microprobes, the ARL-SEMQ at the U.S.G.S. in Reston and the JEOL 733 at Washington University. All analyses were conducted using natural feldspars as standards along with Bence-Albee interelement corrections. An accelerating potential of 15 kV, a beam current of 20 nA, and a de-

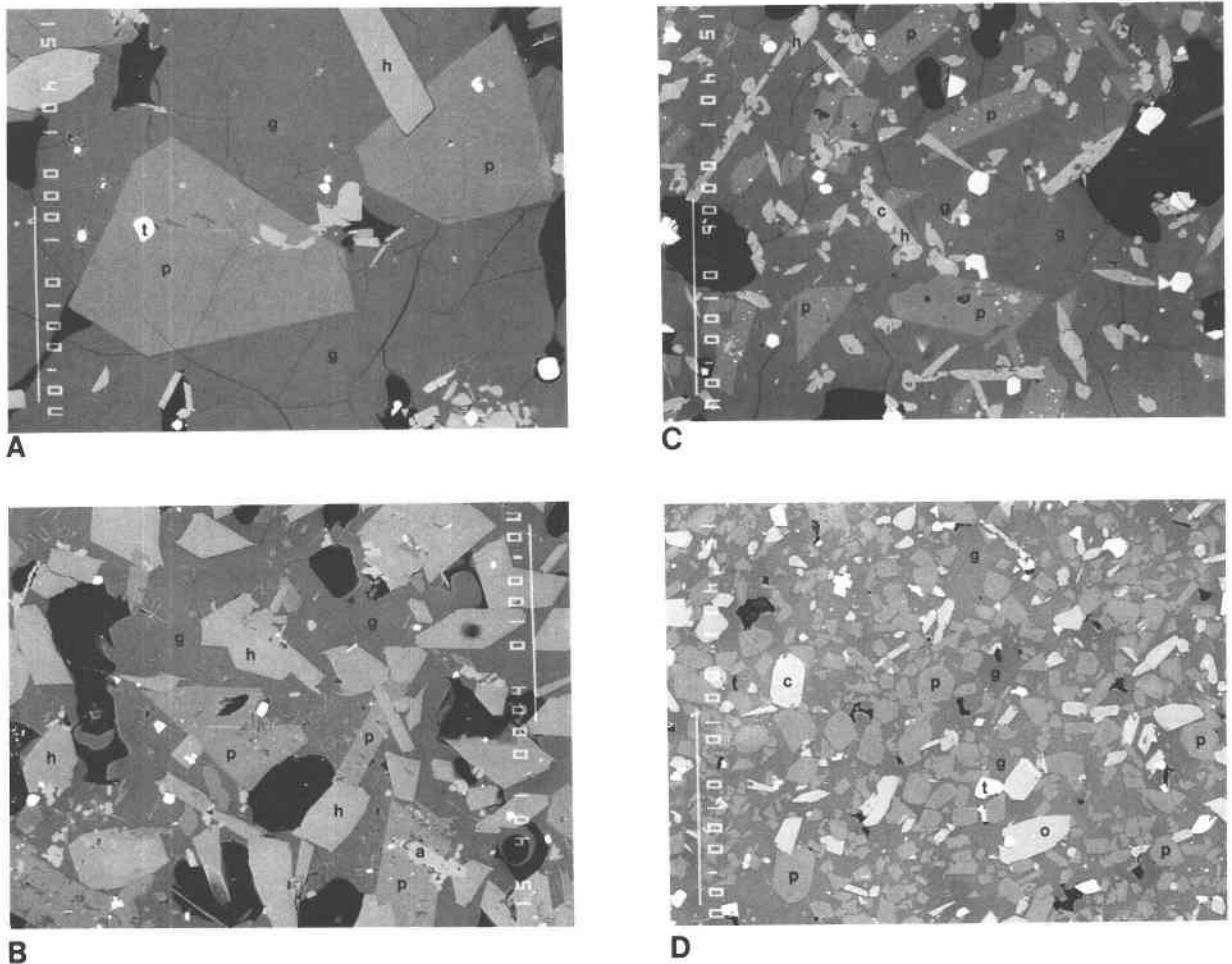


Fig. 1. Backscattered electron photomicrographs of representative plagioclase and glass textures. (A) no. 213, starting composition A1, 850 °C, 4 kbar, MNH buffer; (B) no. 121, starting composition B, 950 °C, 2 kbar, MTH; (C) no. 167, starting composition G, 850 °C, 2 kbar, MNH; (D) no. 285, starting composition A2, 900 °C, 1 kbar, MNH. A 100- μ m scale bar is in the lower left corner of A, C, and D, the upper right in B. Abbreviations of phases: p, plagioclase; g, glass; h, hornblende; t, titanomagnetite; a, anhydrite; c, clinopyroxene; o, orthopyroxene.

focused spot 10 μ m in diameter were used on both probes. On-peak, mean atomic number background corrections were used at Reston, and off-peak background corrections were used at Washington University. In order to assure consistency from experiment to experiment and between the two microprobes, all plagioclase analyses were normalized to an in-experiment standard, a well-analyzed and stoichiometric natural bytownite from Crystal Bay, Minnesota (An_{75.9}). Ten to 12 individual spot analyses were typically collected for plagioclase in each sample. The number of spots analyzed and mean and one standard deviation values are given for each plagioclase in Table 2. Plagioclase is relatively homogeneous in most samples, without any significant variations related to position in the sample or rim-core location in a single crystal. The degree of homogeneity is indicated by the mean of all standard deviations for An content of 3.2 ± 1.5 mol%. In order to test for consistency between the two

microprobes, plagioclases from four samples (nos. 139, 169, 119, 171) were analyzed on each machine (Table 2). These pairs of analyses are very similar, on average differing by only 0.35 mol% An, well within the one standard deviation values.

THE ALBITE-ANORTHITE BINARY PROJECTION

The well-known liquidus-solidus loop for the albite-anorthite system at 1-bar pressure (Bowen, 1913) is shown in Figure 2, along with the loop for 5-kbar H₂O pressure (Yoder et al., 1957). The latter has a very similar shape but is shifted downward in temperature by 350–400 °C. Wyllie (1963) and Morse (1980) showed that when 1-bar plagioclase-melt compositions are projected onto the albite-anorthite binary from the diopside-plagioclase cotectic in the ternary system diopside-albite-anorthite, the liquidus-solidus loop collapses to a very narrow temperature range of approximately 100 °C (Fig. 2). A similar

TABLE 2. Electron microprobe analyses of experimental plagioclase

Sample no.	153	149	105	263	268	218	203	193	144	165
St. Comp.	A1	A1	A1	A1	A1	A1	A1	A1	A1	A1
Hours:	102	48	96	68	43	56	80	60	48	81
T (°C):	800	800	800	800	800	800	800	800	850	850
P (bars):	2000	2000	2000	2500	2500	4000	4000	4000	2000	2000
O ₂ buffer:	FMQ	MNH	MTH	MNH	MTH	FMQ	MNH	MTH	FMQ	MNH
H ₂ O (wt%):	6.02	5.98	5.95	6.52	6.49	8.25	8.24	8.30	6.04	5.99
Mean analyses										
Spots:	11	12	12	10	10	9	10	12	12	12
Probe:	W.U.	U.S.G.S	U.S.G.S	W.U.	W.U.	W.U.	W.U.	W.U.	U.S.G.S	U.S.G.S
SiO ₂	57.09	56.88	56.88	57.50	57.73	56.12	54.62	55.67	54.72	54.81
Al ₂ O ₃	26.65	25.06	26.53	26.67	27.41	28.06	27.93	27.86	27.87	28.01
Fe ₂ O ₃ *	0.44	0.97	0.63	0.45	0.46	0.24	0.44	0.47	0.60	0.69
CaO	8.15	8.97	9.04	8.80	9.22	10.02	10.22	10.07	10.54	10.54
Na ₂ O	6.29	5.91	6.02	5.70	5.52	5.52	5.40	5.60	5.35	5.49
K ₂ O	0.82	0.61	0.68	0.79	0.82	0.41	0.40	0.40	0.40	0.47
Total	99.45	98.40	99.78	99.90	101.16	100.37	99.02	100.07	99.48	100.01
One standard deviation values										
SiO ₂	0.97	0.83	0.88	1.09	1.27	0.39	0.59	0.77	0.54	0.72
Al ₂ O ₃	0.57	0.93	0.43	0.48	0.70	0.36	0.36	0.57	0.75	0.81
Fe ₂ O ₃ *	0.09	0.20	0.09	0.05	0.06	0.03	0.04	0.07	0.06	0.04
CaO	0.73	0.45	0.65	0.55	0.73	0.38	0.44	0.55	0.57	0.75
Na ₂ O	0.42	0.32	0.31	0.19	0.43	0.27	0.21	0.31	0.25	0.37
K ₂ O	0.08	0.09	0.14	0.07	0.17	0.04	0.07	0.10	0.07	0.10
Formulae based on 8 O atoms										
Si	2.578	2.602	2.566	2.582	2.563	2.515	2.489	2.507	2.485	2.479
Al	1.419	1.351	1.411	1.412	1.434	1.483	1.500	1.480	1.492	1.494
Fe	0.015	0.033	0.021	0.015	0.015	0.008	0.015	0.016	0.021	0.023
Ca	0.395	0.439	0.437	0.423	0.438	0.481	0.499	0.486	0.513	0.511
Na	0.551	0.524	0.527	0.496	0.475	0.480	0.477	0.489	0.471	0.482
K	0.047	0.036	0.039	0.045	0.046	0.023	0.023	0.023	0.023	0.027
mol% An	39.7	44.0	43.6	43.9	45.7	48.9	49.9	48.7	50.9	50.1
Sample no.	139	139	228	213	208	185	169	169	114	104
St. Comp.	A1		A1	A1	A1	A1	A1		A1	A1
Hours:	72		46	84	44	15	68		48	72
T (°C):	850		850	850	850	900	900		900	950
P (bars):	2000		4000	4000	4000	2000	2000		2000	2000
O ₂ buffer:	MTH		FMQ	MNH	MTH	FMQ	MNH		MTH	MNH
H ₂ O (wt%):	5.99		8.24	8.19	8.22	6.08	6.05		6.05	5.98
Mean analyses										
Spots:	11	10	10	10	11	10	12	10	11	12
Probe:	U.S.G.S	W.U.	W.U.	W.U.	W.U.	W.U.	U.S.G.S.	W.U.	U.S.G.S.	U.S.G.S.
SiO ₂	55.36	54.69	51.25	50.97	49.86	53.05	51.20	51.71	52.82	48.98
Al ₂ O ₃	27.57	27.49	30.48	29.86	31.02	30.39	29.23	29.75	29.37	31.19
Fe ₂ O ₃ *	0.72	0.74	0.31	0.59	0.54	0.42	0.80	0.81	0.83	1.10
CaO	10.03	10.15	12.93	12.90	12.66	12.30	12.59	12.65	12.15	14.68
Na ₂ O	5.49	5.51	4.05	4.01	4.12	4.39	4.22	4.18	4.61	3.02
K ₂ O	0.49	0.51	0.21	0.21	0.21	0.28	0.29	0.26	0.31	0.17
Total	99.66	99.09	99.22	98.53	98.40	100.82	98.33	99.36	100.10	99.14
One standard deviation values										
SiO ₂	0.67	0.31	0.58	0.67	1.14	0.54	0.62	0.67	0.60	0.66
Al ₂ O ₃	0.54	0.39	0.38	0.58	0.43	0.47	0.54	0.43	0.48	0.60
Fe ₂ O ₃ *	0.04	0.12	0.07	0.08	0.04	0.09	0.04	0.04	0.05	0.06
CaO	0.45	0.31	0.26	0.50	0.46	0.29	0.45	0.44	0.53	0.47
Na ₂ O	0.25	0.18	0.14	0.27	0.33	0.15	0.20	0.24	0.23	0.26
K ₂ O	0.06	0.04	0.03	0.03	0.02	0.03	0.50	0.05	0.05	0.03
Formulae based on 8 O atoms										
Si	2.507	2.495	2.347	2.354	2.307	2.385	2.371	2.368	2.398	2.263
Al	1.472	1.478	1.646	1.625	1.692	1.611	1.596	1.606	1.572	1.699
Fe	0.025	0.025	0.011	0.021	0.019	0.014	0.028	0.028	0.028	0.038
Ca	0.487	0.496	0.635	0.638	0.628	0.592	0.625	0.621	0.591	0.727
Na	0.482	0.488	0.360	0.359	0.369	0.382	0.379	0.371	0.406	0.271
K	0.028	0.030	0.012	0.012	0.012	0.016	0.017	0.015	0.018	0.010
mol% An	48.8	49.0	63.0	63.2	62.2	59.8	61.2	61.6	58.2	72.1

TABLE 2—Continued

Sample no.	119	119	155	152	108	265	270	220	205	195
St. Comp.	A1		B	B	B	B	B	B	B	B
Hours:	36		102	48	96	68	43	56	80	60
T (°C):	950		800	800	800	800	800	800	800	800
P (bars):	2000		2000	2000	2000	2500	2500	4000	4000	4000
O ₂ buffer:	MTH		FMQ	MNH	MTH	MNH	MTH	FMQ	MNH	MTH
H ₂ O (wt%):	5.98		5.95	5.81	5.84	6.43	6.43	8.04	8.12	8.12
Mean analyses										
Spots:	12	9	9	12	12	10	11	10	12	10
Probe:	U.S.G.S.	W.U.	W.U.	U.S.G.S.	U.S.G.S.	W.U.	W.U.	W.U.	W.U.	W.U.
SiO ₂	49.06	49.40	53.60	57.06	56.25	51.93	57.02	56.21	55.60	54.84
Al ₂ O ₃	31.10	30.89	29.10	26.71	27.20	29.30	28.41	28.16	28.25	28.82
Fe ₂ O ₃ *	1.13	1.22	0.45	0.56	0.62	0.58	0.43	0.23	0.37	0.36
CaO	14.87	14.58	11.55	9.04	9.71	12.51	10.36	10.24	10.39	11.08
Na ₂ O	3.06	3.12	4.88	6.32	6.01	4.34	5.35	5.74	5.66	5.37
K ₂ O	0.18	0.17	0.17	0.18	0.19	0.10	0.18	0.15	0.16	0.13
Total	99.41	99.39	99.75	99.87	99.98	98.77	101.75	100.73	100.43	100.60
One standard deviation values										
SiO ₂	0.35	0.45	0.91	0.77	1.93	1.29	1.96	0.76	0.61	0.83
Al ₂ O ₃	0.43	0.14	0.85	0.46	1.11	0.71	0.96	0.31	0.41	0.38
Fe ₂ O ₃ *	0.07	0.04	0.06	0.06	0.13	0.08	0.07	0.03	0.06	0.05
CaO	0.28	0.31	0.72	0.41	1.49	0.90	1.15	0.34	0.43	0.53
Na ₂ O	0.15	0.14	0.40	0.26	0.72	0.48	0.53	0.21	0.33	0.33
K ₂ O	0.02	0.02	0.04	0.05	0.05	0.02	0.04	0.03	0.03	0.02
Formulae based on 8 O atoms										
Si	2.263	2.277	2.431	2.566	2.533	2.387	2.518	2.511	2.495	2.462
Al	1.691	1.679	1.556	1.416	1.444	1.588	1.479	1.483	1.494	1.525
Fe	0.039	0.042	0.015	0.019	0.021	0.020	0.014	0.008	0.012	0.012
Ca	0.735	0.720	0.562	0.435	0.468	0.616	0.490	0.490	0.500	0.533
Na	0.274	0.279	0.430	0.551	0.525	0.387	0.458	0.497	0.493	0.468
K	0.011	0.010	0.010	0.010	0.011	0.006	0.010	0.009	0.009	0.007
mol% An	72.1	71.4	56.1	43.7	46.7	61.1	51.2	49.2	49.9	52.9
Sample no.	146	168	141	230	215	121	156	151	107	148
St. Comp.	B	B	B	B	B	B	G	G	G	G
Hours:	48	81	72	46	84	36	102	48	96	48
T (°C):	850	850	850	850	850	950	800	800	800	850
P (bars):	2000	2000	2000	4000	4000	2000	2000	2000	2000	2000
O ₂ buffer:	FMQ	MNH	MTH	FMQ	MNH	MTH	FMQ	MNH	MTH	FMQ
H ₂ O (wt%):	6.01	5.91	5.88	8.10	8.13	5.89	6.10	6.05	6.00	6.09
Mean analyses										
Spots:	12	12	12	10	11	12	10	12	13	12
Probe:	U.S.G.S.	U.S.G.S.	U.S.G.S.	W.U.	W.U.	U.S.G.S.	W.U.	U.S.G.S.	U.S.G.S.	U.S.G.S.
SiO ₂	53.96	53.91	55.03	52.32	51.77	49.10	58.95	57.92	58.54	55.48
Al ₂ O ₃	28.44	28.42	27.53	29.90	29.97	31.32	26.55	25.05	25.69	27.66
Fe ₂ O ₃ *	0.66	0.77	0.69	0.31	0.53	0.90	0.42	0.70	0.67	0.62
CaO	11.48	11.54	10.59	12.54	12.76	14.95	8.00	8.02	7.72	10.15
Na ₂ O	5.09	5.07	5.35	4.56	4.20	2.95	6.79	6.54	6.92	5.71
K ₂ O	0.15	0.15	0.19	0.10	0.07	0.08	0.87	0.87	0.82	0.41
Total	99.78	99.85	99.38	99.72	99.30	99.30	101.59	99.11	100.36	100.03
One standard deviation values										
SiO ₂	0.66	0.88	1.13	0.67	0.89	1.52	0.59	0.99	0.94	0.67
Al ₂ O ₃	0.37	0.40	0.62	0.54	0.43	1.13	0.47	0.58	0.58	0.47
Fe ₂ O ₃ *	0.07	0.11	0.07	0.05	0.08	0.10	0.05	0.10	0.07	0.10
CaO	0.50	0.58	0.83	0.52	0.30	0.92	0.40	0.55	0.57	0.45
Na ₂ O	0.23	0.33	0.51	0.24	0.17	0.41	0.21	0.24	0.21	0.20
K ₂ O	0.02	0.02	0.04	0.02	0.01	0.04	0.08	0.10	0.16	0.05
Formulae based on 8 O atoms										
Si	2.449	2.446	2.499	2.381	2.368	2.264	2.605	2.626	2.620	2.504
Al	1.521	1.520	1.474	1.604	1.616	1.702	1.383	1.339	1.355	1.472
Fe	0.023	0.026	0.024	0.011	0.018	0.031	0.014	0.024	0.023	0.021
Ca	0.558	0.561	0.515	0.611	0.625	0.739	0.379	0.390	0.370	0.491
Na	0.448	0.446	0.471	0.402	0.373	0.263	0.582	0.575	0.600	0.500
K	0.009	0.009	0.011	0.006	0.004	0.005	0.049	0.050	0.047	0.024
mol% An	55.0	55.3	51.7	60.0	62.4	73.4	37.5	38.4	36.4	48.4

TABLE 2—Continued

Sample no.	167	143	272	222	207	197	232	217	212
St. Comp.	G	G	A2	A2	A2	A2	A2	A2	A2
Hours:	81	72	43	56	80	60	46	84	44
T (°C):	850	850	800	800	800	800	850	850	850
P (bars):	2000	2000	2500	4000	4000	4000	4000	4000	4000
O ₂ buffer:	MNH	MTH	MTH	FMQ	MNH	MTH	FMQ	MNH	MTH
H ₂ O (wt%):	6.06	6.04	6.43	8.12	8.00	7.98	8.09	8.07	8.07
Mean analyses									
Spots:	13	7	10	10	10	12	2	10	10
Probe:	W.U.	W.U.	W.U.	W.U.	W.U.	W.U.	W.U.	W.U.	W.U.
SiO ₂	56.03	56.69	57.39	56.25	55.58	55.88	53.23	52.76	52.68
Al ₂ O ₃	26.95	26.43	26.50	27.75	27.34	27.79	29.94	30.03	29.85
Fe ₂ O ₃ *	0.93	0.81	0.43	0.21	0.39	0.46	0.26	0.60	0.70
CaO	9.95	9.26	8.69	9.69	9.62	9.73	12.26	12.54	12.35
Na ₂ O	5.83	6.25	6.35	5.96	5.87	6.17	4.75	4.58	4.66
K ₂ O	0.53	0.52	0.28	0.17	0.17	0.15	0.15	0.07	0.07
Total	100.21	99.96	99.63	100.03	98.97	100.19	100.59	100.59	100.30
One standard deviation values									
SiO ₂	0.99	1.10	0.83	0.57	0.71	0.57	0.08	0.63	0.51
Al ₂ O ₃	0.68	0.58	0.43	0.42	0.38	0.28	0.23	0.25	0.51
Fe ₂ O ₃ *	0.07	0.07	0.06	0.04	0.07	0.03	0.01	0.04	0.05
CaO	0.59	0.48	0.43	0.41	0.38	0.38	0.27	0.25	0.18
Na ₂ O	0.26	0.27	0.33	0.22	0.27	0.79	0.04	0.15	0.16
K ₂ O	0.07	0.03	0.04	0.02	0.03	0.03	0.00	0.01	0.02
Formulae based on 8 O atoms									
Si	2.527	2.557	2.583	2.527	2.526	2.512	2.399	2.382	2.385
Al	1.432	1.406	1.406	1.470	1.465	1.473	1.590	1.598	1.593
Fe	0.032	0.027	0.015	0.007	0.013	0.016	0.009	0.020	0.024
Ca	0.481	0.447	0.419	0.466	0.468	0.469	0.592	0.606	0.599
Na	0.509	0.547	0.554	0.519	0.517	0.538	0.415	0.401	0.409
K	0.030	0.030	0.016	0.010	0.010	0.009	0.009	0.004	0.004
mol% An	47.1	43.7	42.4	46.9	47.1	46.2	58.3	60.0	59.2
Sample no.	210	187	171	171	116	200	103	289	285
St. Comp.	B	B	B	B	B	B	B	A2	A2
Hours:	44	15	68		48	11.3	72	18	22
T (°C):	850	900	900		900	950	950	900	900
P (bars):	4000	2000	2000		2000	2000	2000	1000	1000
O ₂ buffer:	MTH	FMQ	MNH		MTH	FMQ	MNH	FMQ	MNH
H ₂ O (wt%):	8.07	6.02	5.96		5.91	6.08	5.93	4.09	4.06
Mean analyses									
Spots:	11	10	12	9	12	10	12	10	10
Probe:	W.U.	W.U.	U.S.G.S.	W.U.	U.S.G.S.	W.U.	U.S.G.S.	W.U.	W.U.
SiO ₂	52.90	52.55	52.53	52.56	52.38	50.19	48.81	56.06	54.75
Al ₂ O ₃	29.95	30.41	28.98	29.34	29.53	31.21	31.48	27.35	28.55
Fe ₂ O ₃ *	0.52	0.50	0.73	0.76	0.82	0.56	0.93	0.67	0.68
CaO	12.43	12.50	12.37	12.18	12.65	14.34	15.00	9.86	10.96
Na ₂ O	4.51	4.34	4.57	4.53	4.40	3.44	2.89	6.01	5.39
K ₂ O	0.09	0.11	0.11	0.11	0.11	0.08	0.09	0.22	0.21
Total	100.39	100.41	99.28	99.47	99.88	99.82	99.20	100.17	100.55
One standard deviation values									
SiO ₂	0.45	0.68	0.69	0.29	0.82	0.31	1.16	1.38	1.90
Al ₂ O ₃	0.36	0.36	0.46	0.40	0.56	0.32	0.58	0.95	1.34
Fe ₂ O ₃ *	0.05	0.06	0.04	0.05	0.13	0.04	0.10	0.09	0.06
CaO	0.35	0.50	0.50	0.29	0.66	0.23	0.84	1.04	1.46
Na ₂ O	0.26	0.27	0.22	0.13	0.33	0.08	0.40	0.54	0.81
K ₂ O	0.01	0.02	0.02	0.02	0.02	0.01	0.04	0.05	0.06
Formulae based on 8 O atoms									
Si	2.390	2.374	2.403	2.398	2.384	2.295	2.254	2.523	2.462
Al	1.595	1.619	1.563	1.578	1.584	1.682	1.713	1.451	1.514
Fe	0.018	0.017	0.025	0.026	0.028	0.019	0.032	0.023	0.023
Ca	0.602	0.605	0.606	0.595	0.617	0.703	0.742	0.475	0.528
Na	0.395	0.380	0.405	0.400	0.388	0.305	0.259	0.524	0.470
K	0.005	0.006	0.006	0.006	0.006	0.005	0.005	0.013	0.012
mol% An	60.1	61.0	59.6	59.4	61.0	69.4	73.8	47.0	52.3

Note: St. Comp = starting composition: A1, B, G, and A2 as described in the text. Hours = duration of experiment. O₂ buffer = O buffer used in experiment: FMQ, MNH, and MTH. H₂O = H₂O solubility limit calculated after Burnham and Nekvasil (1986) as described in the text. Spots = number of spot analyses used to calculate mean and one standard deviation values. Probe indicates which microprobe was used in analyzing plagioclase: W.U., JEOL 733 at Washington University; U.S.G.S., ARL SEMQ at Reston, Virginia. The value of mol% An = 100 × [Ca/(Ca + Na + K)].

* Total Fe as Fe₂O₃.

collapse of the plagioclase-melt loop might be expected for projections of natural multicomponent systems. In the lower part of Figure 2, we have plotted the projected positions of 54 experimental plagioclase and glass compositions from this study along with other H₂O-saturated plagioclase-glass pairs from the literature: ten pairs formed at 5-kbar pressure from Helz (1976) and four pairs formed between 1250 bars and 2250 bars from Rutherford et al. (1985). The majority of these experimental data from natural rock compositions form distinct isobaric trends similar in slope to those for the 5-kbar binary system of Yoder et al. (1957). The projected compositions from these multicomponent systems are shifted downward in temperature by approximately 300 °C compared to the binary system, such that the 1-kbar projected data are essentially superimposed on the 5-kbar binary trends. The H₂O-saturated experimental glasses of this study, Rutherford et al. (1985), and Helz (1976) have only 57.8 ± 9.5 wt% normative albite + anorthite, but 92.4 ± 3.9 wt% normative quartz + orthoclase + albite + anorthite. For systems containing large percentages of normative quartz and orthoclase, it appears that plagioclase-glass compositions project onto the albite-anorthite binary with lowered temperatures but without significant distortion of the binary loop topology (but see Johannes, 1984). On the contrary, systems with large percentages of normative diopside (and presumably other mafic constituents) lead to substantial collapse of the liquidus-solidus loop.

The set of 54 plagioclase-glass pairs from this study contains considerable redundancy, owing to the use of three different O buffers and two to four different starting compositions at each temperature-pressure condition. The different O buffers were chosen to investigate effects on S solubility in the melt (Luhr, 1990) and compositional relationships among the melt and mafic minerals; these O buffers should have little influence on plagioclase-melt equilibria. Likewise, the different bulk compositions appear to have no significant effect on the projected plagioclase-melt compositions. The great redundancy of the data set, with up to nine different experiments at a single temperature-pressure condition, allowed us to evaluate each experiment for consistency with the total data set. Plagioclase or glass analyses, or both, from eight of the experiments of this study (nos. 108, 116, 149, 152, 155, 193, 203, 265) fall off of the general compositional trends (Fig. 2: half-closed symbols). Seven of the eight aberrant charges were conducted at 800 °C and are inferred to reflect disequilibrium at this lowest temperature condition. As the slope of the isobaric curves is well defined at higher temperatures, there is little doubt about the expected equilibrium plagioclase and glass compositions at 800 °C. These eight samples have been deleted from the following analysis and from subsequent figures. Although the data of Helz (1976) are plotted on subsequent figures, these too have been deleted from the analysis because they deviate from trends displayed by the data of this study and Rutherford et al. (1985). The possible cause of this deviation is the correction technique applied to ac-

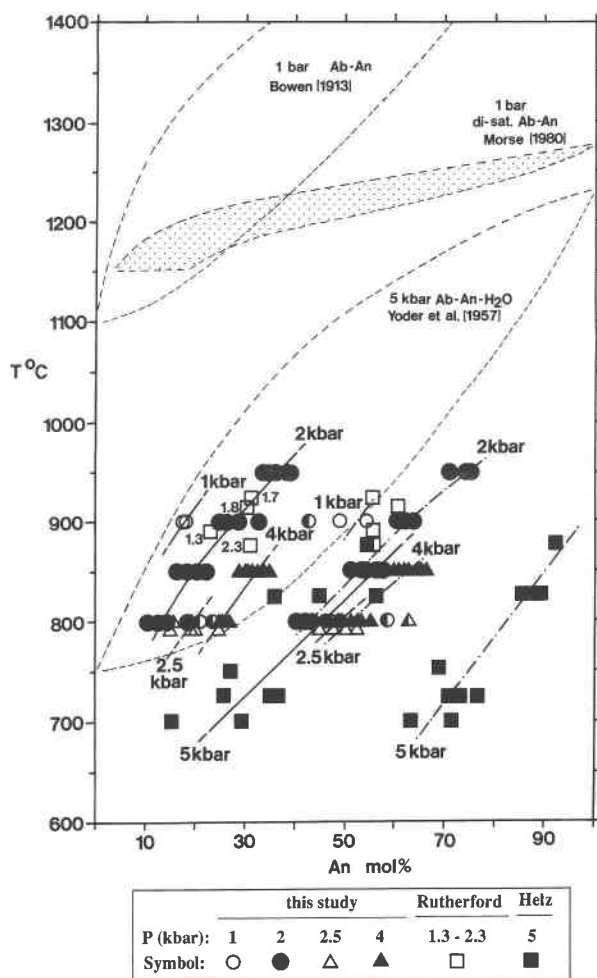


Fig. 2. Albite-anorthite binary diagram showing the 1-bar liquidus-solidus loop of Bowen (1913) and the 5-kbar H₂O-saturated loop of Yoder et al. (1957). Also shown is the collapse of the loop when projected from diopside saturation in the system diopside-albite-anorthite (Wyllie, 1963; Morse, 1980). Symbols show plagioclase and projected glass compositions from this study, Helz (1976), and Rutherford et al. (1985). Multicomponent glass compositions are plotted as 100[normative an/(an + ab)]. Half closed symbols indicate the eight samples whose plagioclase or glass compositions deviate from the general trends and are deleted from the modeling. Small numbers adjacent to open squares indicate experimental pressures in kbar for data from Rutherford et al. (1985). Solid and dash-dot lines labeled 1 kbar, 2 kbar, 2.5 kbar, 4 kbar, and 5 kbar indicate mean loci of projected isobaric melt and plagioclase compositions, respectively.

count for alkali loss in the glass as a result of electron bombardment during the microprobe analysis (Helz, 1976).

THE KUDO-WEILL PLAGIOCLASE GEOTHERMOMETER

In order to emphasize the need for reformulation of plagioclase-melt equilibrium relationships for hydrous

melts, we have plotted in Figure 3 the 60 available H₂O-saturated plagioclase-glass pairs from this study, Helz (1976), and Rutherford et al. (1985) in the form of $y(T)$ vs. T [see Kudo and Weill (1970) for the definition and calculation of $y(T)$]. Also shown are the linear regression curves of Kudo and Weill (1970) and Mathez (1973, 1974) for anhydrous conditions and $P_{\text{H}_2\text{O}} = 0.5$ kbar, 1 kbar, and 5 kbar. Although the 1- to 5-kbar experimental data fall between the 1- and 5-kbar $P_{\text{H}_2\text{O}}$ regression lines, most predicted $P_{\text{H}_2\text{O}}$ values are significantly higher than the experimental values at the given experimental temperature. Several possibilities can be put forward to explain these problems with the Kudo-Weill formulation. First, at the time of their study, the significance of Na loss during electron beam bombardment of hydrous glasses was not well appreciated. Kudo and Weill (1970) do not discuss this problem and do not give the specimen current at which the granitic glasses were analyzed, so this effect is difficult to appraise in their data. Second, as discussed above and pointed out by Wyllie (1963), Loomis (1979), and Morse (1980), plagioclase-melt relationships are dramatically changed when melt compositions lie significantly off the binary. Accordingly, reliance of the Kudo-Weill (1970) formulations on data from simple systems may contribute to its failure when applied to natural multicomponent systems.

PLAGIOCLASE-MELT EQUILIBRIA

We have approached the problem of plagioclase-melt equilibria by solving for the equilibrium constants of exchange reactions for albite and anorthite components between these two phases. Activities of albite and anorthite in plagioclase ($a_{\text{Ab,pl}}$ and $a_{\text{An,pl}}$) were calculated following Lindsley and Nekvasil (1989) and Fuhrman and Lindsley (1988). In treating melt components we have evaluated three different models for silicate melts, which we now discuss in turn: the two-site quasi-lattice model of Nielsen and Dungan (1983), the quasi-crystalline model of Burnham and Nekvasil (1986), and the regular-solution model of Ghiorso et al. (1983).

Two-site quasi-lattice model

We slightly modified the technique of Nielsen and Dungan (1983) to account for the presence of minor MnO and SO₃ in the experimental glasses, and we speciated the glass compositions into network-forming components SiO₂, NaAlO₂, and KAlO₂, and network-modifying components TiO₂, AlO_{1.5}, FeO, MnO, MgO, CaO, and SO₃. Activities of these components in the melt were then taken as equal to the mole fractions on the respective quasi-lattice sites. Each of the 60 H₂O-saturated plagioclase-glass pairs was then used to calculate $\ln K_{\text{Ab}}$ and $\ln K_{\text{An}}$, where

$$\ln K_{\text{Ab}} = \ln a_{\text{Ab,pl}} - \ln X_{\text{NaAlO}_2,\text{NF}} - 3 \ln X_{\text{SiO}_2,\text{NF}}$$

and

$$\ln K_{\text{An}} = \ln a_{\text{An,pl}} - \ln X_{\text{CaO,NF}} - 2 \ln X_{\text{AlO}_{1.5},\text{NM}} - 2X_{\text{SiO}_2,\text{NF}}$$

Figures 4a and 4b show plots of these equilibrium constants vs. reciprocal temperature. As also found by Drake (1976) and Nielsen and Dungan (1983) in the temperature range of this study (<1000 °C), the data of Figure 4 show a systematic increase in $\ln K_{\text{Ab}}$ with reciprocal temperature, but considerable scatter for $\ln K_{\text{An}}$. The poor quality of the anorthite reaction might reflect the fact that Ca is present in both diopside-like and anorthite-like melt molecules, a possibility not accounted for by the two-site quasi-lattice model (Drake, 1976). On Figure 4a, the $\ln K_{\text{Ab}}$ data show separate subparallel trends for the different experimental pressures, with the intercept increasing systematically from 5 kbar to 1 kbar. The systematic lowering of $\ln K_{\text{Ab}}$ with increasing $P_{\text{H}_2\text{O}}$ may reflect the increasing mole fraction of H₂O in the melt. If the concentration of H₂O in the melt could be explicitly accounted for in the model, all data points might collapse onto a single line, as shown later for the regular-solution melt model of Ghiorso et al. (1983). It is not obvious, however, how to adapt the two-site quasi-lattice model to hydrous conditions. The simplest approach is to assume that all H₂O enters the melt on the network-modifying lattice. This will not cause any change in the mole fractions of species on the network-forming site, however, and since both melt-phase albite components are on the network-forming site, this will similarly cause no change in the calculated $\ln K_{\text{Ab}}$. For this reason, the two-site quasi-lattice model was not pursued any further.

Quasi-crystalline model

The quasi-crystalline melt model of Burnham and Nekvasil (1986) was designed to model activity-composition relationships within the system quartz-feldspar-H₂O. As described above, the 60 H₂O-saturated glasses considered in our analysis have >90% normative quartz + feldspars. Accordingly, we modified the method of Burnham and Nekvasil (1986) to accommodate the remaining components. CIPW norms were calculated for each glass. In addition to q, or, ab, and an, the glasses contain normative di, hy, c, mt, il, hm, ru, and wo; S in the glasses was calculated as normative pyrrhotite (po) or anhydrite (anhy) depending upon the O buffer. The normative proportions were converted from wt% to mole fractions and then converted to molecules with eight O atoms (or S atoms for po): 4q, or, an, ab, 8/3c, 8/3hy, dpy, 2mt, 8/3ilm, 8/3hm, 4ru, 8/3wo, 2anhy, and 8po. Normative 8/3c was combined with normative 4q to form dehydroxylated pyrophyllite (dpy) as described by Burnham (1981: Table 9.2). After this normative speciation of the melt, components were combined in three groups: (1) albite-like: ab, an, or, dpy, 2mt, 8/3il, 8/3hm, 8po, 4ru, and 2anhy; (2) quartz-like: 4q; and (3) diopside-like: 4/3di, 8/3hy, and 8/3wo. H₂O contents in the melt were then calculated by summing the contributions of these three groups, treating albite- and quartz-like components as described by Burnham and Nekvasil (1986) and diopside-like components as described by Egger and Burnham (1984). H₂O solubility values calculated in this fash-

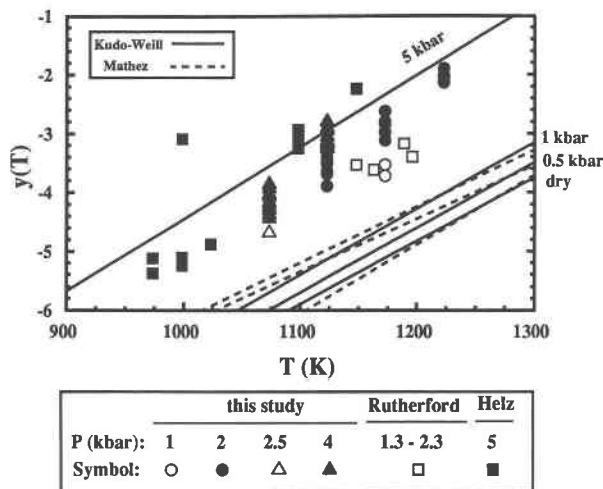


Fig. 3. Plot of Kudo-Weill (1970) parameter $y(T)$ vs. T , showing experimental data of this study (46 pairs), Helz (1976: ten pairs), and Rutherford et al. (1985: four pairs), along with linear regression lines of Kudo and Weill (1970) and Mathez (1973, 1974) for dry conditions and $P_{\text{H}_2\text{O}} = 0.5$ kbar, 1 kbar, and 5 kbar.

ion for the glasses of this study were reported by Luhr (1990) and listed in Table 2; these were used in calculating activity-composition relationships both for the quasi-crystalline model and for the regular-solution model discussed in the following section.

Activities of albite and anorthite in the hydrous melt were calculated as described by Burnham and Nekvasil (1986). First the mole fractions of Ab and An in the anhydrous melt were calculated: $X_{\text{Ab,am}}$ and $X_{\text{An,am}}$. The appropriate eutectic compositions were calculated from Table 2a of Burnham and Nekvasil (1986): $X_{\text{Ab,am}}(\text{E})$ and $X_{\text{An,am}}(\text{E})$. Using Table 2b or 2d of Burnham and Nekvasil (1986), the difference functions $X_{\text{Ab,am}} - a_{\text{Ab,am}}$ and $X_{\text{An,am}} - a_{\text{An,am}}$ were then calculated. From $X_{\text{Ab,am}}$ and $X_{\text{An,am}}$, the corresponding activities in the anhydrous melt were determined. Finally, these anhydrous activities were used to calculate activities of Ab and An in the hydrous melt ($a_{\text{Ab,hm}}$ and $a_{\text{An,hm}}$) from Equations 5 and 6 of Burnham and Nekvasil (1986).

The reaction constants for exchange of albite and anorthite components between plagioclase and melt were then determined as

$$\ln K_{\text{Ab}} = \ln a_{\text{Ab,pl}} - \ln a_{\text{Ab,hm}}$$

and

$$\ln K_{\text{An}} = \ln a_{\text{An,pl}} - \ln a_{\text{An,hm}}$$

These values are plotted in Figure 5 vs. reciprocal temperature, with different symbols distinguishing experimental H_2O pressures. Because the melt model of Burnham and Nekvasil (1986) explicitly accounts for H_2O , all data points should collapse onto a single line. This is clearly not the case. The data of Helz (1976) are systematically shifted to higher $\ln K$ values as compared to the

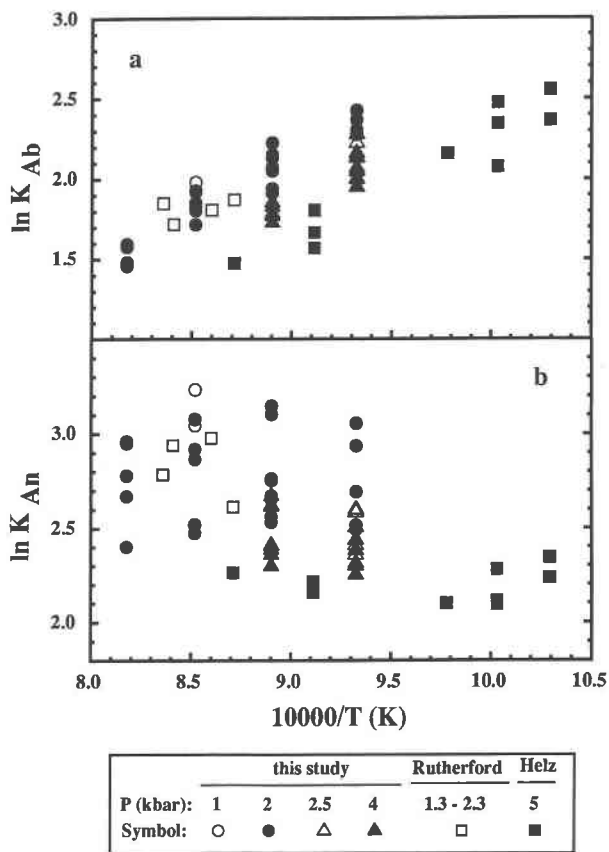


Fig. 4. Equilibrium constants for albite (a) and anorthite (b) plotted vs. reciprocal temperature, with melt components calculated according to the two-site quasi-lattice model of Nielsen and Dungan (1983).

other data and are not included in the regression. Among the remaining data of this study and Rutherford et al. (1985), deviations from the regression lines are not systematically related to H_2O pressure or f_{O_2} (not shown). The standard errors of the regressions (109.7 K for $\ln K_{\text{Ab}}$, 75.5 K for $\ln K_{\text{An}}$) are quite large compared to those achieved with the regular-solution melt model described next.

Regular-solution model

In applying the regular-solution melt model of Ghiorso et al. (1983), we first subtracted CaO or Fe from the glass analysis to balance the analyzed S as either anhydrite or pyrrhotite, depending upon the O buffer. These minor components were not considered in the calculation. The remaining oxide components were then normalized to 100- H_2O , the latter being the H_2O solubility value (in wt%) calculated according to Burnham and Nekvasil (1986), as described above. These wt% oxide components were then converted to molecular proportions and speciated into the eight O-atom molecules of Ghiorso et al. (1983; Table 4). Activity coefficients for the components $\text{Na}_{16/3}\text{Si}_{8/3}\text{O}_8$, $\text{Ca}_4\text{Si}_2\text{O}_8$, and Si_4O_8 in the hydrous melt were

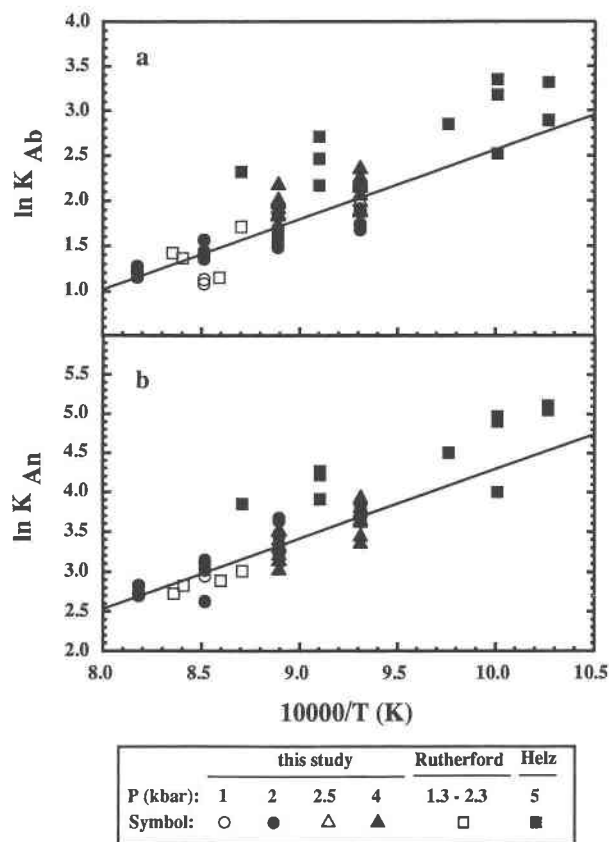


Fig. 5. Equilibrium constants for albite (a) and anorthite (b) plotted vs. reciprocal temperature, with melt components calculated according to the quasi-crystalline model of Burnham and Nekvasil (1986). Regression equations for the 50 plagioclase-glass pairs of this study and Rutherford et al. (1985): $\ln K_{Ab} = -5.054 + 7597.7(1/T)$, $R^2 = 0.689$, standard error of 109.7 K; $\ln K_{An} = -4.546 + 8845.4(1/T)$, $R^2 = 0.824$, standard error of 75.5 K.

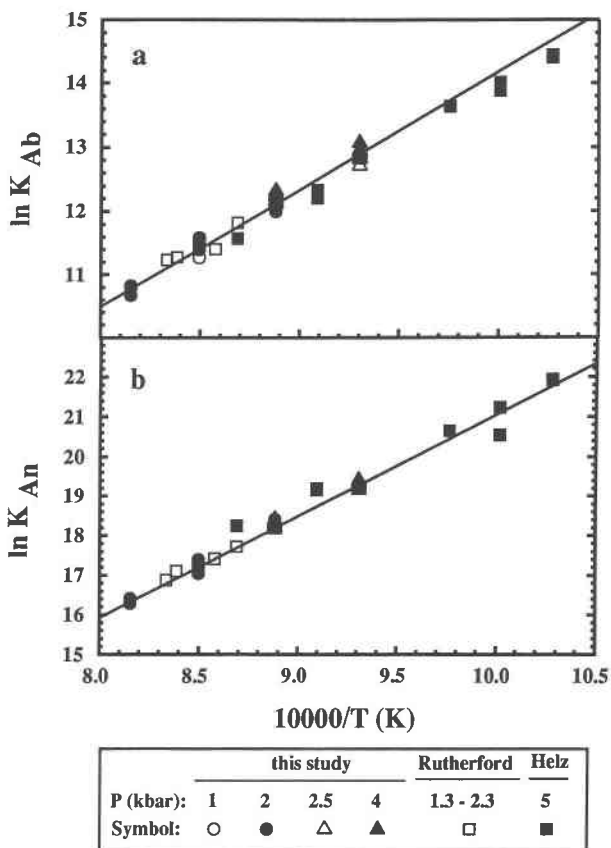


Fig. 6. Equilibrium constants for albite (a) and anorthite (b) plotted vs. reciprocal temperature, with melt components calculated according to the regular-solution model of Ghiorso et al. (1983). Regression equations for the 50 plagioclase-glass pairs of this study and Rutherford et al. (1985): $\ln K_{Ab} = -4.365 + 18571.1(1/T)$, $R^2 = 0.984$, standard error of 20.6 K; $\ln K_{An} = -4.627 + 25689.8(1/T)$, $R^2 = 0.993$, standard error of 13.4 K.

calculated from Equation A3-16 using the binary interaction parameters from Table A4-3 of Ghiorso et al. (1983). Activities for these components are simply the product of the mole fractions in the hydrous melt and the activity coefficients. Combined with the activities of Ab and An in plagioclase, these values were used to evaluate the reaction constants

$$\ln K_{Ab} = \ln a_{Ab,pl} - \frac{3}{16} \ln a_{Na_{16}/3Si_8/3O_8} - \frac{3}{16} \ln a_{Al_{16}/3O_8} - \frac{5}{8} \ln a_{Si_4O_8} \quad (1)$$

$$\ln K_{An} = \ln a_{An,pl} - \frac{1}{4} \ln a_{Ca_4Si_2O_8} - \frac{3}{8} \ln a_{Al_{16}/3O_8} - \frac{3}{8} \ln a_{Si_4O_8} \quad (2)$$

These expressions are plotted vs. reciprocal temperature in Figure 6, with symbols distinguishing different exper-

imental H_2O pressures. Again, deviations are noted for the data of Helz (1976). For both expressions, the remaining 50 H_2O -saturated experimental data points conform closely to a single line. Regression parameters are given in Figure 6. The quality of the regression fits (standard errors: 20.6 K for $\ln K_{Ab}$, 13.4 K for $\ln K_{An}$) indicates that the regular-solution formulation is highly successful in modeling activity-composition relationships in hydrous silicate melts.

In order to illustrate the universality of the albite and anorthite exchange reactions formulated with the regular-solution melt model, in Figure 7 we plot the 60 H_2O -saturated data considered earlier along with 15 H_2O -undersaturated plagioclase-glass pairs from Baker and Egglar (1987) and 76 pairs from 1-bar anhydrous experiments (Grove and Bryan, 1983; Sack et al., 1987). The plot of $\ln K_{Ab}$ vs. reciprocal temperature in Figure 7a shows a strong linear correlation for all data, with a standard error for these 140 data points of 12.1 K. The plot of $\ln K_{An}$ vs. reciprocal temperature in Figure 7b shows somewhat

more scatter, especially at higher temperatures. In this plot, the 1-bar data appear to define a slightly different trend from the hydrous data. Nonetheless, the standard error for the 140 data points is just 15.2 K.

In the following section, we apply the regular-solution melt model to the problem of determining the H₂O contents of melts from compositions of coexisting plagioclase and glass in volcanic rocks.

ESTIMATION OF H₂O CONTENTS

The reaction constants plotted in Figure 7 were calculated using the compositions of coexisting plagioclase and glass determined with an electron microprobe and the experimental H₂O solubility values calculated after Burnham and Nekvasil (1986). Typically, however, the H₂O content of a natural melt is not known, and thus the reaction constant cannot be correctly calculated. In this section we examine the effect of the H₂O content of a melt upon the evaluation of plagioclase-melt equilibria using the melt solution model of Ghiorso et al. (1983) and the plagioclase activity model of Lindsley and Nekvasil (1989) and Fuhrman and Lindsley (1988).

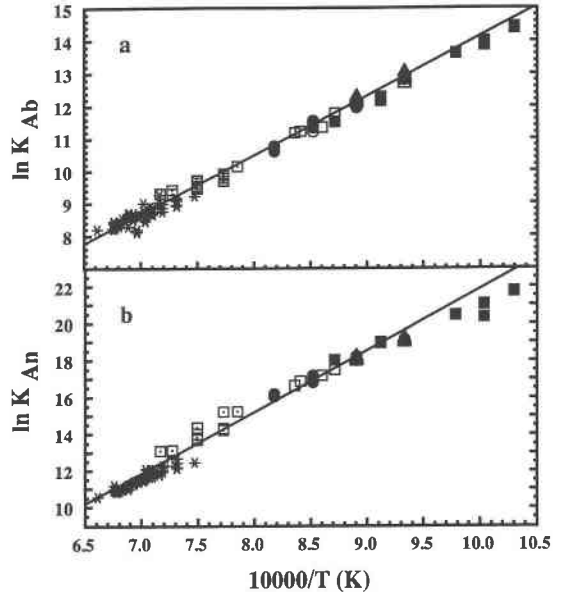
The H₂O content of a melt affects the reaction constants of Equations 1 and 2 through its effect on the activities of the melt components Na_{1/6/3}Si_{8/3}O₈, Ca₄Si₂O₈, Al_{1/6/3}O₈, and Si₄O₈. The activities of these components are calculated by multiplying the mole fractions of the components by their respective activity coefficients which, for a hydrous melt, are given by:

$$RT \ln \gamma_k = \sum_{i=1}^n W_{k,i} X_i - \frac{1}{2} \sum_{i=1}^n \sum_{j=1}^n W_{i,j} X_i X_j + RT \ln(1 - X_w) \quad (3)$$

(Eq. A3-16; Ghiorso et al., 1983), where γ_k is the activity coefficient of melt component k , X_i is the mole fraction (calculated on a hydrous basis) of component i , $W_{i,j}$ is the binary interaction coefficient between components i and j , and X_w is the mole fraction of H₂O in the melt. Since the H₂O content of the melt is unknown, the hydrous mole fractions must be converted into anhydrous mole fractions using the relationship: $X_i = X'_i(1 - X_w)$, where X'_i is the mole fraction of component i calculated on an anhydrous basis. The activity of component i in the melt thus becomes

$$a_i = X'_i(1 - X_w)$$

$$\cdot \exp \left\{ \frac{1}{RT} \left[\sum_{i \neq \text{H}_2\text{O}} W_{k,i} X'_i(1 - X_w) + W_{k,\text{H}_2\text{O}} X_w - \frac{1}{2} \sum_{i \neq \text{H}_2\text{O}} \sum_{j \neq \text{H}_2\text{O}} W_{i,j} X'_i X'_j (1 - X_w)^2 - \sum_{j=1}^n W_{\text{H}_2\text{O},j} X_w X'_j (1 - X_w) + RT \ln(1 - X_w) \right] \right\} \quad (4)$$



	this study		Rutherford	Helz	Sack & Grove	Baker & Egger
P (kbar):	1	2, 2.5, 4	1.3 - 2.3	5	0.001	2-5 undersat.
Symbol:	○	●, △, ▲	□	■	*	□

Fig. 7. Equilibrium constants for albite (a) and anorthite (b) plotted vs. reciprocal temperature, with melt components calculated according to the regular-solution model of Ghiorso et al. (1983). Plots include the 60 H₂O-saturated data points of Figure 6, along with the H₂O-undersaturated data of Baker and Egger (1987: 15 pairs, 1.7–2.0 wt% H₂O in melt, $P_{\text{tot}} = 2$ and 5 kbar), and the 1-bar anhydrous data of Grove and Bryan (1983: 30 pairs) and Sack et al. (1987: 45 pairs); the 1-bar data are collectively labeled "Sack and Grove." Regression equations for entire data set, with 140 plagioclase-glass pairs: $\ln K_{\text{Ab}} = -4.059 + 18213.9(1/T)$, $R^2 = 0.993$, standard error of 12.1 K; $\ln K_{\text{An}} = -11.488 + 33388.6(1/T)$, $R^2 = 0.989$, standard error of 15.2 K.

The relationships between temperature and X_w for plagioclase-melt equilibria can be determined by substituting into Equations 1 and 2 the following: (a) Equation 4, (b) the analytical expressions for $a_{\text{Ab,pl}}$ and $a_{\text{An,pl}}$ (Fuhrman and Lindsley, 1988; Lindsley and Nekvasil, 1989), and (c) the relationship: $\ln K = m \cdot (1/T) + b$, where m and b are the regression coefficients from the plots of $\ln K_{\text{Ab}}$ and $\ln K_{\text{An}}$ vs. reciprocal temperature (Fig. 6). If we make these substitutions and solve for temperature, we find

$$T(\text{K}, \text{Ab}) = [A + B(1 - X_w)^2 - C(1 - X_w) - m_{\text{Ab}} + X_w(1 - X_w)D - X_w E] / [F + 2 \ln(1 - X_w)] \quad (5)$$

$$T(\text{K}, \text{An}) = [G + B(1 - X_w)^2 - H(1 - X_w) - m_{\text{An}} + X_w(1 - X_w)D - X_w I] / [J + 2 \ln(1 - X_w)] \quad (6)$$

The terms in these expressions are

$$A = \frac{1}{R} \{ (W_{\text{OrAb}}^{\text{H}} + P W_{\text{OrAb}}^{\text{V}}) [2 X_{\text{Ab}}^{\text{pl}} X_{\text{Ab}}^{\text{gl}} (1 - X_{\text{Ab}}^{\text{pl}})] \}$$

$$\begin{aligned}
& + X_{Or}^{pl} X_{An}^{pl} \left(\frac{1}{2} - X_{Ab}^{pl} \right) \\
& + (W_{AbOr}^H + PW_{AbOr}^V) [(X_{Or}^{pl})^2 (1 - 2X_{Ab}^{pl}) \\
& \quad + X_{Or}^{pl} X_{An}^{pl} \left(\frac{1}{2} - X_{Ab}^{pl} \right)] \\
& + (W_{OrAn}^H + PW_{OrAn}^V) [X_{Or}^{pl} X_{An}^{pl} \left(\frac{1}{2} - X_{Ab}^{pl} - 2X_{An}^{pl} \right)] \\
& + (W_{AnOr}^H + PW_{AnOr}^V) [X_{Or}^{pl} X_{An}^{pl} \left(\frac{1}{2} - X_{Ab}^{pl} - 2X_{Or}^{pl} \right)] \\
& + (W_{AbAn}^H + PW_{AbAn}^V) [(X_{An}^{pl})^2 (1 - 2X_{Ab}^{pl}) \\
& \quad + X_{Or}^{pl} X_{An}^{pl} \left(\frac{1}{2} - X_{Ab}^{pl} \right)] \\
& + (W_{AnAb}^H + PW_{AnAb}^V) [2X_{Ab}^{pl} X_{An}^{pl} (1 - X_{Ab}^{pl}) \\
& \quad + X_{Or}^{pl} X_{An}^{pl} \left(\frac{1}{2} - X_{Ab}^{pl} \right)] \\
& + (W_{OrAbAn}^H + PW_{OrAbAn}^V) [X_{Or}^{pl} X_{An}^{pl} (1 - 2X_{Ab}^{pl})]
\end{aligned}$$

where X_{Ab}^{pl} , X_{An}^{pl} , and X_{Or}^{pl} are the mole fractions of albite, anorthite, and orthoclase, respectively, in the plagioclase, and W^H and W^V are the binary and ternary interaction coefficients for the plagioclase components,

$$B = \frac{1}{2R} \sum_{i=1}^n \sum_{j=1}^n W_{ij} X_i' X_j'$$

$$\begin{aligned}
C = \frac{1}{R} \left[\frac{3}{16} \sum_{i=1}^n W_{Na_{16}/3Si_8/3O_8, i} X_i' + \frac{3}{16} \sum_{i=1}^n W_{Al_{16}/3O_8, i} X_i' \right. \\
\left. + \frac{5}{8} \sum_{i=1}^n W_{Si_4O_8, i} X_i' \right]
\end{aligned}$$

$$D = \frac{1}{R} \sum_{j=1}^n W_{H_2O, j} X_j'$$

$$\begin{aligned}
E = \frac{1}{R} \left[\frac{3}{16} W_{Na_{16}/3Si_8/3O_8, H_2O} + \frac{3}{16} W_{Al_{16}/3O_8, H_2O} \right. \\
\left. + \frac{5}{8} W_{Si_4O_8, H_2O} \right]
\end{aligned}$$

$$\begin{aligned}
F = b_{Ab} + \frac{3}{16} \ln X'_{Na_{16}/3Si_8/3O_8} + \frac{3}{16} \ln X'_{Al_{16}/3O_8} \\
+ \frac{5}{8} \ln X'_{Si_4O_8} - \ln X_{Ab}^{pl} \\
+ \frac{1}{R} \{ W_{OrAb}^S [2X_{Ab}^{pl} X_{Or}^{pl} (1 - X_{Ab}^{pl}) \\
+ X_{Or}^{pl} X_{An}^{pl} \left(\frac{1}{2} - X_{Ab}^{pl} \right)]
\end{aligned}$$

$$\begin{aligned}
& + W_{AbOr}^S [(X_{Or}^{pl})^2 (1 - 2X_{Ab}^{pl}) + X_{Or}^{pl} X_{An}^{pl} \left(\frac{1}{2} - X_{Ab}^{pl} \right)] \\
& + W_{OrAn}^S [X_{Or}^{pl} X_{An}^{pl} \left(\frac{1}{2} - X_{Ab}^{pl} - 2X_{An}^{pl} \right)] \\
& + W_{AnOr}^S [X_{Or}^{pl} X_{An}^{pl} \left(\frac{1}{2} - X_{Ab}^{pl} - 2X_{Or}^{pl} \right)] \\
& + W_{AbAn}^S [(X_{An}^{pl})^2 (1 - 2X_{Ab}^{pl}) + X_{Or}^{pl} X_{An}^{pl} \left(\frac{1}{2} - X_{Ab}^{pl} \right)] \\
& + W_{AnAb}^S [2X_{Ab}^{pl} X_{An}^{pl} (1 - X_{Ab}^{pl}) \\
& \quad + X_{Or}^{pl} X_{An}^{pl} \left(\frac{1}{2} - X_{Ab}^{pl} \right)] \\
& + W_{OrAbAn}^S [X_{Or}^{pl} X_{An}^{pl} (1 - 2X_{Ab}^{pl})]
\end{aligned}$$

$$\begin{aligned}
G = \frac{1}{R} \{ (W_{OrAb}^H + PW_{OrAb}^V) [X_{Ab}^{pl} X_{Or}^{pl} \left(\frac{1}{2} - X_{An}^{pl} - 2X_{Ab}^{pl} \right)] \\
+ (W_{AbOr}^H + PW_{AbOr}^V) [X_{Ab}^{pl} X_{Or}^{pl} \left(\frac{1}{2} - X_{An}^{pl} - 2X_{Or}^{pl} \right)] \\
+ (W_{OrAn}^H + PW_{OrAn}^V) [2X_{Or}^{pl} X_{An}^{pl} (1 - X_{An}^{pl}) \\
+ X_{Ab}^{pl} X_{Or}^{pl} \left(\frac{1}{2} - X_{An}^{pl} \right)] \\
+ (W_{AnOr}^H + PW_{AnOr}^V) [(X_{Or}^{pl})^2 (1 - 2X_{An}^{pl}) \\
+ X_{Ab}^{pl} X_{Or}^{pl} \left(\frac{1}{2} - X_{An}^{pl} \right)] \\
+ (W_{AbAn}^H + PW_{AbAn}^V) [2X_{Ab}^{pl} X_{An}^{pl} (1 - X_{An}^{pl}) \\
+ X_{Ab}^{pl} X_{Or}^{pl} \left(\frac{1}{2} - X_{An}^{pl} \right)] \\
+ (W_{AnAb}^H + PW_{AnAb}^V) [(X_{An}^{pl})^2 (1 - 2X_{An}^{pl}) \\
+ X_{Ab}^{pl} X_{Or}^{pl} \left(\frac{1}{2} - X_{An}^{pl} \right)] \\
+ (W_{OrAbAn}^H + PW_{OrAbAn}^V) [X_{Or}^{pl} X_{Ab}^{pl} (1 - 2X_{An}^{pl})]
\end{aligned}$$

$$\begin{aligned}
H = \frac{1}{R} \left[\frac{1}{4} \sum_{i=1}^n W_{Ca_4Si_2O_8, i} X_i' + \frac{3}{8} \sum_{i=1}^n W_{Al_{16}/3O_8, i} X_i' \right. \\
\left. + \frac{3}{8} \sum_{i=1}^n W_{Si_4O_8, i} X_i' \right]
\end{aligned}$$

$$\begin{aligned}
I = \frac{1}{R} \left[\frac{1}{4} W_{Ca_4Si_2O_8, H_2O} + \frac{3}{8} W_{Al_{16}/3O_8, H_2O} \right. \\
\left. + \frac{3}{8} W_{Si_4O_8, H_2O} \right]
\end{aligned}$$

$$J = b_{An} + \frac{1}{4} \ln X'_{Ca_4Si_2O_8} + \frac{3}{8} \ln X'_{Al_{16}/3O_8}$$

$$\begin{aligned}
& + \frac{3}{8} \ln X'_{\text{Si4O8}} - \ln X_{\text{An}}^{\text{pl}} \\
& + \frac{1}{R} \{ W_{\text{OrAb}}^S [X_{\text{Ab}}^{\text{pl}} X_{\text{Or}}^{\text{pl}} (\frac{1}{2} - X_{\text{An}}^{\text{pl}} - 2X_{\text{Ab}}^{\text{pl}})] \\
& \quad + W_{\text{AbOr}}^S [X_{\text{Ab}}^{\text{pl}} X_{\text{Or}}^{\text{pl}} (\frac{1}{2} - X_{\text{An}}^{\text{pl}} - 2X_{\text{Or}}^{\text{pl}})] \\
& \quad + W_{\text{OrAn}}^S [2X_{\text{Or}}^{\text{pl}} X_{\text{An}}^{\text{pl}} (1 - X_{\text{An}}^{\text{pl}}) \\
& \quad \quad + X_{\text{Ab}}^{\text{pl}} X_{\text{Or}}^{\text{pl}} (\frac{1}{2} - X_{\text{An}}^{\text{pl}})] \\
& \quad + W_{\text{AnOr}}^S [(X_{\text{Or}}^{\text{pl}})^2 (1 - 2X_{\text{An}}^{\text{pl}}) \\
& \quad \quad + X_{\text{Ab}}^{\text{pl}} X_{\text{Or}}^{\text{pl}} (\frac{1}{2} - X_{\text{An}}^{\text{pl}})] \\
& \quad + W_{\text{AbAn}}^S [2X_{\text{Ab}}^{\text{pl}} X_{\text{An}}^{\text{pl}} (1 - X_{\text{An}}^{\text{pl}}) \\
& \quad \quad + X_{\text{Ab}}^{\text{pl}} X_{\text{Or}}^{\text{pl}} (\frac{1}{2} - X_{\text{An}}^{\text{pl}})] \\
& \quad + W_{\text{AnAb}}^S [(X_{\text{Ab}}^{\text{pl}})^2 (1 - 2X_{\text{An}}^{\text{pl}}) \\
& \quad \quad + X_{\text{Ab}}^{\text{pl}} X_{\text{Or}}^{\text{pl}} (\frac{1}{2} - X_{\text{An}}^{\text{pl}})] \\
& \quad + W_{\text{OrAbAn}}^S [X_{\text{Or}}^{\text{pl}} X_{\text{Ab}}^{\text{pl}} (1 - 2X_{\text{An}}^{\text{pl}})] \}.
\end{aligned}$$

For given melt and plagioclase compositions, Equations 5 and 6 define the temperature-H₂O content relationship for the system (a Basic program that calculates these relationships is available from the authors upon request).

If an independent estimate of the temperature for the system can be made (e.g., coexisting Fe-Ti oxides), then the H₂O content of the melt can be determined. Similarly, if the H₂O content of the melt is known, then the temperature can be determined. We have calculated the H₂O contents of the 46 experimental product samples reported here, and in Rutherford et al. (1985) and Helz (1976), using Equations 5 and 6 and the experimental temperatures. These calculated H₂O contents are plotted in Figure 8 against the H₂O solubility values calculated after Burnham and Nekvasil (1986), as discussed previously. The agreement between the H₂O contents is good, except for the samples of Helz (1976). An estimate of the uncertainty associated with these calculations of H₂O content can be made if we assume that the reduced chi-squared (χ^2_r) equals one for the remaining 50 charges and solve for the appropriate σ . This results in approximate uncertainties (1σ) of 0.54 and 0.33 wt% for the H₂O contents of melts as determined by the albite (Eq. 5) and anorthite (Eq. 6) equilibria, respectively.

Equations 5 and 6 have also been used to estimate the H₂O contents of melts from four natural samples: rhyodacite pumice from the climatic eruption of Mount Mazama; dacitic pumice from the May 18, 1980, eruption of Mount St. Helens; the Fish Canyon Tuff; and the trachyandesite pumice from the 1982 eruption of El Chichón.

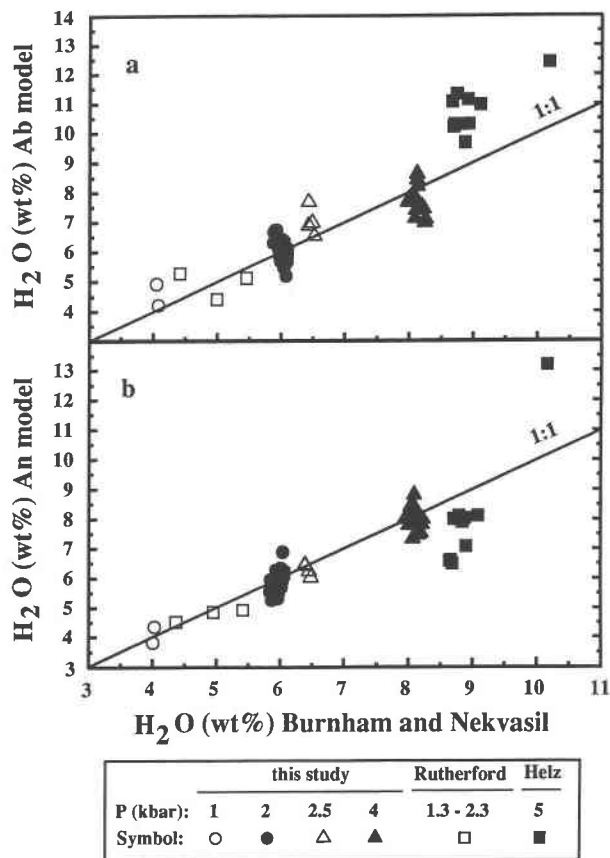


Fig. 8. Melt H₂O contents calculated using Equations 5 and 6 for albite (a) and anorthite (b) plotted vs. H₂O solubility values calculated after Burnham and Nekvasil (1986) as discussed in the text.

The results of these calculations are summarized in Table 3.

Bacon and Druitt (1988) and Druitt and Bacon (1989) reported analyses of matrix glass and plagioclase for rhyodacitic pumices from the climactic eruption of Mount Mazama, and Druitt and Bacon (1989) reported preruptive temperatures between 880 and 886 °C based on coexisting Fe-Ti oxide compositions. Plagioclase compositions within the rhyodacitic pumices varied widely from An₃₂ to An₆₄, although most were less than An₄₀ (Druitt and Bacon, 1989). Using a plagioclase composition of An₃₅, the calculated H₂O contents of the melt are 3.7 wt% (Eq. 5) and 4.3 wt% (Eq. 6), and agree within error. Bacon et al. (1988) examined glass inclusions within plagioclase phenocrysts using infrared spectroscopy and reported a preruptive H₂O content of approximately 4.5 wt% for the melt, easily within 1σ error of the 4.3 wt% calculated using Equation 6 and just over 1σ error from the 3.7 wt% calculated using Equation 5.

Rutherford et al. (1985) published analyses of matrix glass and glass inclusions in plagioclase from the tephra of the May 18, 1980 eruption of Mount St. Helens and

TABLE 3. Calculated H₂O contents for volcanic rocks

	Remarks	T (°C)	H ₂ O (Eq. 5)	H ₂ O (Eq. 6)	H ₂ O (estimated)
Mount Mazama	An ₃₅ *, mg**	883	3.7	4.3	4.5
Mount St. Helens	An ₄₉ , gi	930	3.7	2.7	3.4-4.3
	An ₅₃ , gi	930	4.0	2.5	3.4-4.3
	An ₅₇ , gi	930	4.3	2.3	3.4-4.3
	An ₄₉ , mg	930	3.7	2.9	3.4-4.3
	An ₅₃ , mg	930	4.0	2.7	3.4-4.3
Fish Canyon Tuff	An ₅₇ , mg	930	4.3	2.5	3.4-4.3
	sample 4†	730	6.2	4.7	4-6
	sample 4†	760	5.0	3.9	4-6
El Chichón	sample 4†	790	4.1	3.3	4-6
	An ₃₆ , mg	750	7.9	8.7	6-8
	An ₄₃ , mg	750	8.4	8.1	6-8
	An ₄₉ , mg	750	9.0	7.7	6-8
	An ₃₆ , mg	800	6.0	7.1	6-8
	An ₄₃ , mg	800	6.5	6.6	6-8
	An ₄₉ , mg	800	7.0	6.2	6-8
	An ₃₆ , mg	850	4.5	5.8	6-8
	An ₄₃ , mg	850	5.0	5.3	6-8
	An ₄₉ , mg	850	5.4	4.9	6-8

Note: Sources of data: Mount Mazama: Bacon and Druitt (1988), Druitt and Bacon (1989), Bacon et al. (1988); Mount St. Helens: Rutherford et al. (1985), Merzbacher and Egger (1984); Fish Canyon Tuff: Whitney and Stormer (1985), Johnson and Rutherford (1989); El Chichón: Luhr et al. (1984), Rye et al. (1984).

* Composition of plagioclase used.

** gi: glass inclusion; mg: matrix glass.

† Plagioclase and glass compositions of sample 4 (Whitney and Stormer, 1985).

estimated the preeruptive temperature as 930 °C based on coexisting Fe-Ti oxide compositions and experimental phase relations. They also reported that plagioclase compositions within these samples vary from An₄₉ to An₅₇. Depending upon the plagioclase composition used, the calculated H₂O content of the melt (at 930 °C) ranges from 3.7 to 4.3 wt% (Eq. 5) and 2.3 to 2.9 wt% (Eq. 6). These calculations illustrate the influence of variable plagioclase compositions in natural samples upon the calculated H₂O content of the melt. For plagioclase of composition An₄₉, the calculated H₂O contents for both the matrix glass and melt inclusions of 3.7 wt% (Eq. 5) and 2.7 to 2.9 wt% (Eq. 6) overlap at the 2σ uncertainty. Rutherford et al. (1985) used the difference technique (100% - Σoxides) for the glass inclusions to estimate the total volatile content (H₂O + CO₂) of the Mount St. Helens magma as 4.6 wt%, and based on experimentally determined phase relationships, they estimated that $P_{H_2O}/(P_{H_2O} + P_{CO_2})$ was 0.5 to 0.7. Using the thermodynamic data for H₂O from Burnham et al. (1969) and the melt-H₂O activity relations of Burnham (1981) and Egger and Burnham (1984), the $P_{H_2O}/(P_{H_2O} + P_{CO_2})$ values for the Mount St. Helens magma convert to approximately 3.4 to 4.3 wt% H₂O in the melt, which is broadly consistent with the range of values calculated using Equations 5 and 6. Similarly, Merzbacher and Egger (1984) estimated H₂O contents of 3 to 4 wt% for pyroclastic rocks from the May 1980 eruption of Mount St. Helens by experimentally calibrating the shift of projected cotectics with increasing H₂O content.

Whitney and Stormer (1985) published analyses of the

matrix glass and coexisting plagioclase from the Fish Canyon Tuff. Johnson and Rutherford (1989), using the data of Whitney and Stormer (1985), estimated that preeruptive temperatures were 760 ± 30 °C based on coexisting Fe-Ti oxide compositions. This uncertainty in the temperature produces a range of calculated H₂O contents of the melt from 4.1 to 6.1 wt% (Eq. 5) and 3.3 to 4.7 wt% (Eq. 6). The two calculated H₂O contents best agree at 790 °C (4.1 wt%, calculated from Eq. 5; 3.3 wt%, calculated from Eq. 6). Whitney and Stormer (1985) estimated H₂O contents of melts of the Fish Canyon Tuff between 4 and 6 wt%, based on comparison of observed mineral assemblages in the tuff with published phase relations. Similarly, Johnson and Rutherford (1989) conducted phase equilibrium experiments on a sample of the Fish Canyon Tuff and estimated the H₂O content of the natural melt as 5 wt%.

Luhr et al. (1984) published compositions of matrix glass and plagioclase from the 1982 trachyandesite pumice from El Chichón. For this case, relatively large uncertainties exist in both the equilibrium plagioclase composition and in the preeruptive temperature. The preeruptive temperature was estimated as between 750 and 850 °C using stable isotope partitioning relationships (Rye et al., 1984). The best agreement between the calculated H₂O contents was produced using the dominant plagioclase composition (An₄₃), which yielded relatively high H₂O contents in the melt, between 5.0 and 8.4 wt% depending upon the temperature used. These estimates are consistent with H₂O contents in the melt of 6-8 wt% based on electron microprobe totals for glass inclusions of 93.5 wt% (Luhr et al., 1984) and on experimental phase-equilibria constraints that indicate approximate H₂O saturation at approximately 2 kbar pressure (Carroll and Rutherford, 1987; Luhr, 1990).

CONCLUSIONS

We have modeled H₂O-saturated plagioclase-melt equilibria by evaluating the equilibrium constants of exchange reactions for albite and anorthite components between plagioclase and melt for 46 new experimental charges in the pressure range of 1-4 kbar as well as for data from the literature. Equilibrium constants were calculated using the plagioclase activity-composition model of Fuhrman and Lindsley (1988) and Lindsley and Nekvasil (1989), as well as three different silicate melt solution models: the two-site quasi-lattice model of Nielson and Dungan (1983), the quasi-crystalline model of Burnham and Nekvasil (1986), and the regular-solution model of Ghiorso et al. (1983). Of these melt models, the regular-solution model of Ghiorso et al. (1983) was the most successful in that it resulted in the lowest standard errors for regressions of ln K vs. reciprocal temperature. This model was successfully extended to include published anhydrous and H₂O-undersaturated experimental data.

Not surprisingly, plagioclase-melt equilibria were shown to be strongly dependent upon temperature and the H₂O

content of the melt. The activities of the melt components were calculated using the experimental H₂O contents, a parameter not generally known for natural samples. For this reason, expressions are presented that relate the temperature of the system to the mole fraction of H₂O in the melt for both albite and anorthite equilibria, which allow the H₂O content of the melt to be estimated if the temperature of the system is known. The application of these expressions to the experimental data suggests that these calculations have associated uncertainties on the calculated H₂O contents of approximately 0.54 and 0.33 wt% (1 σ) for the albite and anorthite equilibria, respectively.

Four examples of the calculation of H₂O contents of melts are presented using natural samples. The complexities of these natural samples as reflected in large uncertainties in preeruptive temperature, or compositionally complex plagioclase, or both, may result in a large range of calculated H₂O contents. Successful application of these relationships requires both a good estimate of preeruptive temperature and knowledge of the equilibrium plagioclase and melt compositions.

ACKNOWLEDGMENTS

The experimental work on which this study is based could not have been performed without the kindness and encouragement of Tren Haselton, Rosalind Helz, Bob Rye, Gary Cygan, Steve Huebner, Phil Bethke, I.-M. Chou, and many other U.S.G.S. scientists. Jim McKee (U.S.G.S., Reston) and Dan Kremser (Washington University) offered valuable advice during microprobe analysis. Reviews by Mark Ghiorsio and Allen Glazner are sincerely appreciated. This work was supported by NSF grants EAR-8414946 and EAR-8618872.

REFERENCES CITED

- Bacon, C.R., and Druitt, T.H. (1988) Compositional evolution of the zoned calcalkaline magma chamber of Mount Mazama, Crater Lake, Oregon. *Contributions to Mineralogy and Petrology*, 98, 224–256.
- Bacon, C.R., Newman, S., and Stolper, E. (1988) Preeruptive volatile content, climatic eruption of Mount Mazama, Crater Lake, Oregon. *Geological Society of America Abstracts with Programs*, 20, A248.
- Baker, D.R., and Egger, D.H. (1987) Compositions of anhydrous and hydrous melts coexisting with plagioclase, augite, and olivine or low-Ca pyroxene from 1 atm to 8 kbar: Application to the Aleutian volcanic center of Atka. *American Mineralogist*, 72, 12–28.
- Bowen, N.L. (1913) The melting phenomena of the plagioclase feldspars. *American Journal of Science*, 35, 577–599.
- (1915) The crystallization of haplobasaltic, haplodioritic, and related magmas. *American Journal of Science*, 40, 161–185.
- Burnham, C.W. (1981) The nature of multicomponent aluminosilicate melts. *Physics and Chemistry of the Earth*, 13/14, 197–229.
- Burnham, C.W., and Nekvasil, H. (1986) Equilibrium properties of granite pegmatite magmas. *American Mineralogist*, 71, 239–263.
- Burnham, C.W., Holloway, J.R., and Davis, N.F. (1969) Thermodynamic properties of water to 1,000 °C and 10,000 bars. *Geological Society of America Special Paper* 132, 96 p.
- Carroll, M.R., and Rutherford, M.J. (1987) The stability of igneous anhydrite: Experimental results and implications for sulfur behaviour in the 1982 El Chichón trachyandesite and other evolved magmas. *Journal of Petrology*, 28, 5, 781–801.
- Conrad, W.K., Nicholls, I.A., and Wall, V.J. (1988) Water-saturated and undersaturated melting of metaluminous and peraluminous crustal compositions at 10 kb: Evidence for the origin of silicic magmas in the Taupo Volcanic Zone, New Zealand, and other occurrences. *Journal of Petrology*, 29, 4, 765–803.
- Drake, M.J. (1976) Plagioclase-melt equilibria. *Geochimica et Cosmochimica Acta*, 40, 457–465.
- Druitt, T.H., and Bacon, C.R. (1989) Petrology of the zoned calcalkaline magma chamber of Mount Mazama, Crater Lake, Oregon. *Contributions to Mineralogy and Petrology*, 101, 245–259.
- Egger, D.H., and Burnham, C.W. (1984) Solution of H₂O in diopside melts: A thermodynamic model. *Contributions to Mineralogy and Petrology*, 85, 58–66.
- Fuhrman, M.I., and Lindsley, D.H. (1988) Ternary-feldspar modelling and thermometry. *American Mineralogist*, 73, 201–215.
- Ghiorsio, M.S., Carmichael, I.S.E., Rivers, M.L., and Sack, R.O. (1983) The Gibbs free energy of mixing of natural silicate liquids; an expanded regular solution approximation for the calculation of magmatic intensive variables. *Contributions to Mineralogy and Petrology*, 84, 107–145.
- Glazner, A.F. (1984) Activities of olivine and plagioclase components in silicate melts and their application to geothermometry. *Contributions to Mineralogy and Petrology*, 88, 260–268.
- Grove, T.L., and Bryan, W.B. (1983) Fractionation of pyroxene-phyric MORB at low pressure: An experimental study. *Contributions to Mineralogy and Petrology*, 84, 293–309.
- Helz, R.T. (1976) Phase relations of basalts in their melting ranges at PH₂O = 5 kb. Part II. Melt compositions. *Journal of Petrology*, 17, 139–193.
- Johannes, W. (1984) Beginning of melting in the granite system Qz-Or-Ab-An-H₂O. *Contributions to Mineralogy and Petrology*, 86, 264–273.
- Johnson, M.C., and Rutherford, M.J. (1989) Experimentally determined conditions in the Fish Canyon Tuff, Colorado, magma chamber. *Journal of Petrology*, 30, 711–737.
- Kudo, A.M., and Weill, D.F. (1970) An igneous plagioclase thermometer. *Contributions to Mineralogy and Petrology*, 25, 52–65.
- Lindsley, D.H., and Nekvasil, H. (1989) A ternary feldspar model for all reasons. *Eos*, 70, 506.
- Loomis, T.P. (1979) An empirical model for plagioclase equilibrium in hydrous melts. *Geochimica et Cosmochimica Acta*, 43, 1753–1759.
- Luhr, J.F. (1990) Experimental phase relations of water- and sulfur-saturated arc magmas and the 1982 eruptions of El Chichón Volcano. *Journal of Petrology*, 31, 1071–1114.
- Luhr, J.F., and Carmichael, I.S.E. (1985) Jorullo Volcano, Michoacán, Mexico (1759–1774): The earliest stages of fractionation in calc-alkaline magmas. *Contributions to Mineralogy and Petrology*, 90, 142–161.
- (1990) Petrological monitoring of cyclical eruptive activity at Volcán Colima, Mexico. *Journal of Volcanology and Geothermal Research*, 42, 235–260.
- Luhr, J.F., Carmichael, I.S.E., and Varekamp, J.C. (1984) The 1982 eruptions of El Chichón Volcano, Chiapas, Mexico: Mineralogy and petrology of the anhydrite-bearing pumices. *Journal of Volcanology and Geothermal Research*, 23, 69–108.
- Mathez, E.A. (1973) Refinement of the Kudo-Weill plagioclase thermometer and its application to basaltic rocks. *Contributions to Mineralogy and Petrology*, 41, 61–72.
- (1974) Erratum: Refinement of the Kudo-Weill plagioclase thermometer and its application to basaltic rocks. *Contributions to Mineralogy and Petrology*, 44, 172.
- Merzbacher, C., and Egger, D. (1984) A magmatic geohygrometer: Application to Mount St. Helens and other dacitic magmas. *Geology*, 12, 587–590.
- Morse, S.A. (1980) *Basalts and phase diagrams*, 493 p. Springer-Verlag, New York.
- Nielsen, R.L., and Dungan, M.A. (1983) Low pressure mineral-melt equilibria in natural anhydrous mafic systems. *Contributions to Mineralogy and Petrology*, 84, 310–326.
- Prince, A.T. (1943) The system albite-anorthite-sphene. *Journal of Geology*, 51, 1–18.
- Rutherford, M.J., Sigurdsson, H., Carey, S., and Davis, A. (1985) The May 18, 1980 eruption of Mount St. Helens I. Melt composition and experimental phase equilibria. *Journal of Geophysical Research*, 90, 2929–2947.
- Rye, R.O., Luhr, J.F., and Wasserman, M.D. (1984) Sulfur and oxygen isotope systematics of the 1982 eruptions of El Chichón Volcano, Chia-

- pas, Mexico. *Journal of Volcanology and Geothermal Research*, 23, 109–123.
- Sack, R.O., Walker, D., and Carmichael, I.S.E. (1987) Experimental petrology of alkalic lavas: Constraints on cotectics of multiple saturation in natural basic liquids. *Contributions to Mineralogy and Petrology*, 96, 1–23.
- Smith, M.P. (1983) A feldspar-liquid geothermometer. *Geophysical Research Letters*, 10, 3, 193–195.
- Whitney, J.A., and Stormer, J.C. (1985) Mineralogy, petrology, and magmatic conditions from the Fish Canyon Tuff, central San Juan Volcanic Field, Colorado. *Journal of Petrology*, 26, 726–762.
- Wyllie, P.J. (1963) Effects on the changes in slope occurring on liquidus and solidus paths in the system diopside-anorthite-albite. *Mineralogical Society of America Special Paper* 1, 204–212.
- Yoder, H.S., Stewart, D.B., and Smith, J.R. (1957) Ternary feldspars. *Carnegie Institution of Washington Year Book*, 56, 206–214.

MANUSCRIPT RECEIVED MAY 3, 1990

MANUSCRIPT ACCEPTED JANUARY 14, 1991